

# A Positive Pressure Universal Gripper Based on the Jamming of Granular Material

John R. Amend, Jr., *Student Member, IEEE*, Eric Brown, Nicholas Rodenberg, Heinrich M. Jaeger, and Hod Lipson, *Member, IEEE*

**Abstract**—We describe a simple passive universal gripper, consisting of a mass of granular material encased in an elastic membrane. Using a combination of positive and negative pressure, the gripper can rapidly grip and release a wide range of objects that are typically challenging for universal grippers, such as flat objects, soft objects, or objects with complex geometries. The gripper passively conforms to the shape of a target object, then vacuum-hardens to grip it rigidly, later utilizing positive pressure to reverse this transition—releasing the object and returning to a deformable state. We describe the mechanical design and implementation of this gripper and quantify its performance in real-world testing situations. By using both positive and negative pressure, we demonstrate performance increases of up to 85% in reliability, 25% in error tolerance, and the added capability to shoot objects by fast ejection. In addition, multiple objects are gripped and placed at once while maintaining their relative distance and orientation. We conclude by comparing the performance of the proposed gripper with others in the field.

**Index Terms**—End effectors, grain size, jamming, manipulators, pressure control.

## I. INTRODUCTION

UNIVERSAL robot grippers are robotic end effectors that can grip a wide variety of arbitrarily shaped objects. Proposed universal grippers have ranged from vacuum-based suction grippers to multifingered hands, and these can be divided

Manuscript received January 31, 2011; revised July 19, 2011; accepted September 27, 2011. Date of publication January 31, 2012; date of current version April 9, 2012. This paper was recommended for publication by Associate Editor K. Iagnemma and Editor B. J. Nelson upon evaluation of the reviewers' comments. This work was supported by a National Science Foundation Graduate Research Fellowship and by the Defense Advanced Research Projects Agency, Defense Sciences Office, under the Programmable Matter program Grant W911NF-08-1-0140.

J. R. Amend, Jr. is with the Sibley School of Mechanical and Aerospace Engineering, Cornell University, Ithaca, NY 14853 USA (e-mail: jra224@cornell.edu).

E. Brown was with the James Franck Institute and the Department of Physics, University of Chicago, Chicago, IL 60637 USA. He is now with the School of Natural Sciences, University of California, Merced, CA, USA (e-mail: eric.brown@ucmerced.edu).

H. M. Jaeger is with the James Franck Institute and the Department of Physics, University of Chicago, Chicago, IL 60637 USA (e-mail: hjaeger@uchicago.edu).

N. Rodenberg was with the James Franck Institute and the Department of Physics, University of Chicago, Chicago, IL 60637 USA. He is now with Boston Dynamics, Waltham, MA 02451-7507 USA (e-mail: rodenberg@uchicago.edu).

H. Lipson is with the Sibley School of Mechanical and Aerospace Engineering and the Faculty of Computing and Information Science, Cornell University, Ithaca, NY 14853 USA (e-mail: hod.lipson@cornell.edu).

Color versions of one or more of the figures in this paper are available online at <http://ieeexplore.ieee.org>.

Digital Object Identifier 10.1109/TRO.2011.2171093



Fig. 1. A universal jamming gripper is able to grip a wide variety of objects without grasp planning or sensory feedback. Multiple objects can be gripped at once, as demonstrated here with salt and pepper shakers.

along a spectrum from active universal grippers to passive universal grippers [1].

Most active universal grippers typically have an anthropomorphic multifingered design with many independently actuated joints. Many such grippers have been developed, and multifingered grasping is an active area of research [2]. The active universal grippers that have been proposed are capable of both grasping and manipulation but also engender extensive physical and computational complexity, which is evident in grasp algorithm research [3]–[5]. The complexities of active universal grippers, coupled with their correspondingly high costs, have limited their adoption among commercial robotics industries.

Passive universal grippers [6]–[8] require minimal grasp planning. They often have ten or more degrees of freedom (DOF) per actuator and include components that passively conform to unique object geometries, giving them the ability to grip widely varying objects without readjustment. For example, Scott [6] presented a gripper design in which many independent telescoping pins could each passively slide in or out to conform to the shape of a target object, before pinching from the side to grip the object.

Passive universal grippers are generally simpler to use and require minimal visual preprocessing of their environment, but they too have had limited success gaining widespread adoption.

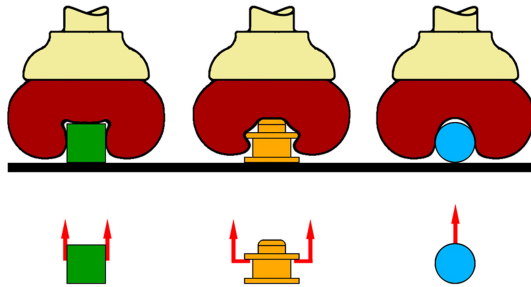


Fig. 2. A universal jamming gripper can achieve three separate gripping modes. (Left) Static friction from surface contact. (Center) Geometric constraints from interlocking. (Right) Vacuum suction from an airtight seal. Normally, it would be unlikely that the interlocking or vacuum modes would be achieved without some additional contribution from friction.

Often, their many passive components are easy to damage and difficult to replace. Passive universal grippers can be very expensive as well, and their ability to grip many different objects often renders them inferior at gripping any one object in particular (a mechanical *no free lunch* [9]).

The term *underactuated* [10] describes universal grippers falling somewhere between the active and passive distinctions. There are no clear dividing lines on this spectrum, but underactuated grippers [11]–[18] are in many ways comparable with passive universal grippers, especially when they possess many more DOF than actuators.

Lower thresholds of universal gripping can be achieved by adding deformable materials to the gripping faces of a traditional 1-DOF jawed gripper in order to increase the compliance of the surfaces [19]–[21]. This technique is straightforward and can be sufficient for some applications. Simpson [22] was likely the first to suggest adding pockets of granular materials to gripping surfaces for this purpose, and later Schmidt [23] and Perovskii [24] proposed designs that allowed vacuum hardening of similar grain filled pockets to produce a custom gripper jaw shape. Reinmueller and Weissmantel [25], while describing a similar idea, went so far as to speculate that a single membrane filled with granular material might be able to grip an object on its own and function as a passive universal gripper. However, this idea was not demonstrated in practice or rigorously explored until the universal jamming gripper that we have recently presented [26].

The approach that we propose in this paper is to use both positive and negative pressure to modulate the jamming transition in a universal jamming gripper. We design, manufacture, and test a prototype gripper that attaches to a commercial robot arm. Consisting of a single mass of granular material encased in an elastic membrane, the gripper can passively conform to the shape of the target object, then vacuum-harden to grip it rigidly, later using positive pressure to reverse this transition—releasing the object and returning to a deformable state. An example of this gripper can be seen in Fig. 1.

This universal jamming gripper is an example of a passive universal gripper that exploits the temperature-independent fluid-like to solid-like phase transition of granular materials known as *jamming* [27]–[32]. This gripper leverages three possible gripping modes for operation: 1) static friction from surface contact; 2) geometric constraints from capture of the object by interlock-

ing; and 3) vacuum suction when an airtight seal is achieved on some portion of the object’s surface [26]. These three gripping modes are illustrated in Fig. 2. The friction force results from the slight ( $<0.5\%$ ) volume contraction of the membrane that occurs during evacuation, which, in turn, causes a pinch force to develop, normal to the point of contact. Analytical calculations for these values have been previously presented [26].

By achieving one or more of the three gripping modes, the jamming gripper can grip many different objects with widely varying shape, weight, and fragility, including objects that are traditionally challenging for other universal grippers. For example, we have successfully been able to grip a coin, a tetrahedron, a hemisphere, a raw egg, a jack toy, and a foam earplug. When mounted to the robot arm, the gripper functions entirely in open loop—without grasp planning, vision, or sensory feedback.

Optimal performance of a universal jamming gripper is maintained by resetting the gripper to a neutral state between gripping tasks. Prior to the work presented here, this was accomplished by shaking the gripper, by kneading or massaging the gripper, or by pushing the gripper against some resetting apparatus that was mounted in the workspace, for example. We call this process *manually resetting the gripper*, and without it, the ability to grip subsequent objects degrades rapidly. We have found that positive pressure can be used to replace this procedure with a short burst of air that quickly unjams and resets the gripper. We also find that incorporating positive pressure improves the gripper’s speed, reliability, error tolerance, and placement accuracy. In addition, the fast ejection that positive pressure can provide enables the gripper to launch objects a significant distance—a capability that we call *shooting*, which may serve as a new method for robots to extend their workspace and perform tasks like sorting objects into bins in a factory or throwing away trash in a home.

In this paper, we develop a new universal jamming gripper that incorporates positive pressure. We quantify the gripper’s ability to grip objects of different shapes and sizes, as well as its ability to tolerate errors in the location of the target object; we test the gripper’s maximum speed and placement precision; we test the gripper’s ability to grip multiple objects at once and to shoot objects of varying weight and shape. Our testing reveals the capabilities and limitations of the gripper, and we compare these with a manual reset gripper in order to isolate the performance contribution from positive pressure. We demonstrate that dramatic improvements in performance are possible through the addition of positive pressure, and we compare the performance of a positive pressure jamming gripper with related grippers in the field. We conclude that this gripper has potential applications in a variety of settings.

## II. DESIGN AND MANUFACTURE

In its simplest form, a jamming gripper needs only to include some granular material that is contained in a flexible membrane in order to achieve its gripping behavior (the combination of ground coffee and a latex balloon has been found to work well [26]). No motors, cables, or linkages are required (just an off-board pump to evacuate the air from the gripper). Here, we

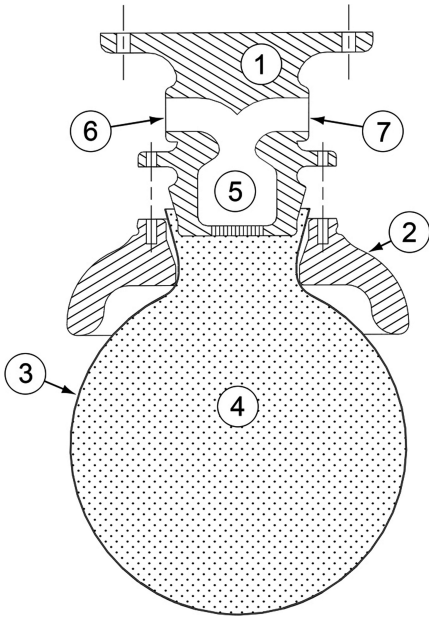


Fig. 3. Assembly drawing of the positive pressure jamming gripper, including components: 1) base, 2) external collar, 3) balloon membrane, 4) coffee grains, 5) air filter, 6) vacuum line port, and 7) high pressure port. The balloon is pinched between the base and the collar producing an airtight seal.

have developed a slightly more complex jamming gripper that interfaces with a commercial robot arm and includes a rigid collar surrounding the membrane, as well as a positive pressure port and an air filter. An assembly drawing of the design is shown in Fig. 3.

One of the primary benefits of this design is its mechanical simplicity. The gripper is composed of just 12 components (the seven shown in Fig. 3 plus five machine screws). This contributes to its low cost and easy manufacturability. The collar is an important element of the design because it helps guide the gripper as it conforms to an object, increasing the surface contact on vertical faces of the object and maximizing the potential for the interlocking gripping mode. In this prototype, the collar and the base are both manufactured from 3-D printed plastic, which permits the intricate internal structures of the base.

The latex balloon membrane is pinched between the base and the collar producing an airtight seal. The balloon membrane thickness is 0.33 mm, and it is filled with ground coffee beans to a volume of  $350 \text{ cm}^3$ . At this volume, the gripper is full but the membrane is not significantly stretched; therefore, the gripper can be easily deformed in the unjammed state. The gripper is approximately spherical, with a radius of 43 mm. The relatively low density of ground coffee is advantageous because it can be used in larger quantities without weighing down the gripper or straining the membrane in the way that a heavier material like sand would, for example.

### III. PERFORMANCE

The jamming gripper was mounted on a commercial robot arm for testing. Positive pressure was provided at 620 kPa and a flow rate of 2.16 L/s. Vacuum was achieved with an off-board vacuum pump. A maximum vacuum flow rate of 0.25

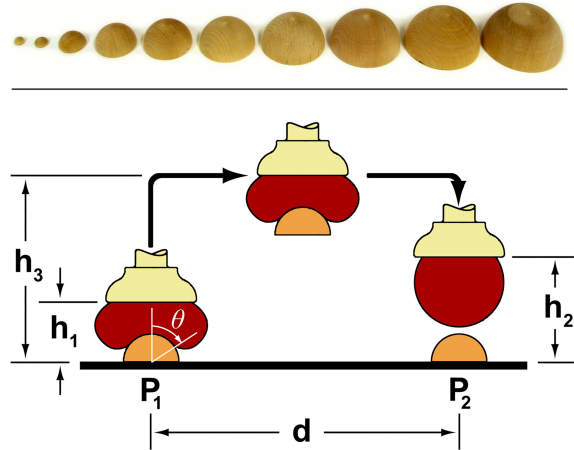


Fig. 4. Hemispheres used in this test ranging from 5-mm radius to 38-mm radius (left to right at top). Experimental setup showing key dimensions (bottom). The gripper picks the object at the pick location ( $P_1$ ) and then moves to place the object at the place location ( $P_2$ ). The contact angle between the gripper and the object is indicated by  $\theta$ .

L/s was achieved with a pump rated for a maximum vacuum of 25 microns. For gripping, the jamming transition was considered complete when the pressure in the gripper dropped to  $-85 \text{ kPa}$ , which took 1.1 s. The pressure in the gripper could also be neutralized with the atmosphere, and this state was used whenever the gripper was pressed onto an object. Solenoid valves that are controlled by serial communication through the robot arm were used to modulate the pressure in the gripper. All tests were performed at 100% joint angle speed for the robot arm, which corresponds to approximately 240 mm/s linear speed of the gripper. When the manual reset gripper was tested, a 2 s massage was given between each gripping task to return it to a uniform neutral state. This setup was used throughout the following subsections, except where otherwise noted.

#### A. Size and Reliability

The positive pressure jamming gripper was first evaluated for its reliability in gripping objects of varying size. All objects were located at a position on a table that was hard-coded into the robot's software (the pick position). The robot was instructed to move to the pick position and press the jamming gripper onto an object and to then actuate the gripper to induce the rigid state. Next, the robot was instructed to move to a place position, release the vacuum, and apply a 0.1 s burst of positive pressure to eject the object. All tests were performed in open loop.

Spheres have been used as test objects for jamming grippers [26], but here, we have chosen to use hemispheres (oriented flat side down) so that the surface geometry of a sphere test would be preserved, but the height of the test objects would be reduced. Wooden hemispheres ranging from 5 mm radius to 38 mm radius were chosen, with a surface texture that was not smooth enough to permit an airtight seal between the gripper and the hemisphere, therefore, not inducing the vacuum mode of gripping. Since the objects are hemispheres, it is also impossible to achieve the interlocking gripping mode in this test. Each hemisphere was located in line with the central axis of the

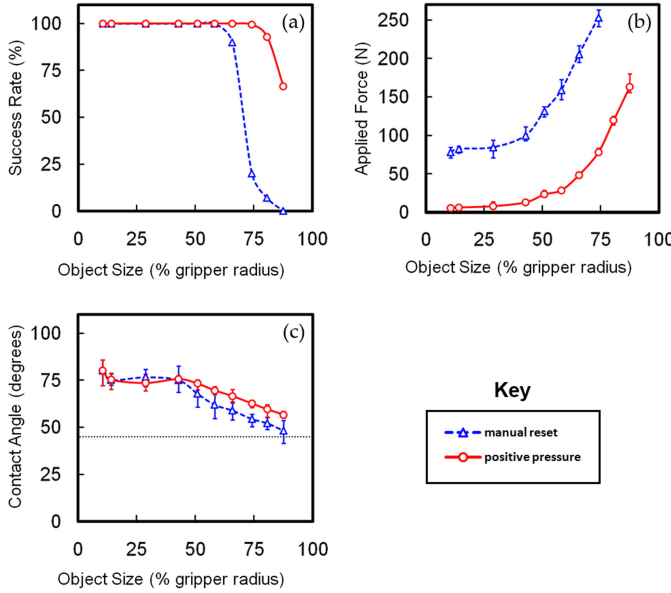


Fig. 5. Results of gripping tests on hemispheres of varying radius using a manually reset gripper and a gripper reset with positive pressure. (a) Success rate for gripping objects of varying size. (b) Force that the gripper applies to an object while deforming around it. (c) Contact angle that the gripper achieves. The horizontal dotted line in (c) indicates the critical  $45^\circ$  contact angle.

gripper so that the contact angle  $\theta$  would be as consistent as possible around the hemisphere. The test setup and the hemispheres that are used for this test can be seen in Fig. 4. The dimensions associated with Fig. 4 were as follows:  $h_1 = 48$  mm,  $h_2 = 115$  mm,  $h_3 = 130$  mm, and  $d = 200$  mm.

Test results are shown in Fig. 5. The ordinate of each plot is presented as a percentage of the gripper size in order to account for the scalability of the gripper [26]. Fig. 5 shows the performance of the new positive pressure gripper compared with a manually reset gripper. Plots of success rate, applied force, and contact angle are shown. Success rate was determined over 30 trials for each hemisphere and represents how reliably the grippers could grip hemispheres of varying size. Applied force is the maximum force that a gripper applies to an object as it is deformed around it. This force is measured with a scale that is located beneath the test object. Contact angle is the maximum angle at which the gripper membrane and the object touch (as indicated by  $\theta$  in Fig. 4). Contact angle was measured with the gripper pressed against the hemisphere and evacuated but before the hemisphere was lifted. For the applied force and contact angle tests, ten trials were performed on each hemisphere. For all three plots, the data points represent the average of the trials, and the error bars indicate the maximum and minimum measurements that are recorded during the test. Hemispheres were tested in random order for all tests.

It can be seen that for a gripper without positive pressure, the gripper's success rate falls off sharply as the object radius reaches about 65% of the gripper radius and falls to 0% for contact angles near  $45^\circ$  (i.e., the critical angle for gripping to occur [26]). No minimum object radius was observed in this test, although no hemispheres under 5 mm radius were tested because of their lack of availability in wood. We also see that the applied force increases with increasing object size, as more grains inside

the gripper need to be displaced around larger objects. Adding positive pressure dramatically increases the success rate of the gripper by as much as 85% for some hemispheres by increasing contact angle. Positive pressure also decreases the force that is applied to the object by as much as 90%. These performance increases are most likely because of increased fluidization of the granular material, which allows it to flow more easily around the target object.

### B. Error Tolerance

In this second test, the jamming gripper was evaluated for tolerance to errors in the location of the target object. The same test setup from Fig. 4 was used, with hemispheres that are again employed as test objects. In this test, however, the target object was located between 0 and 45 mm away from the pick location  $P_1$ , thus, causing the hemisphere to be unaligned with the gripper's central axis. Results from this test are shown in Fig. 6. In Fig. 6(a), only results for the 25 mm radius hemisphere are shown, and 30 trials were performed for each data point. We can observe an increased error tolerance of up to 25% from the addition of positive pressure. Fig. 6(b) illustrates a more general relationship between target object size, location error, and gripping success rate, and ten trials were performed for each data point shown, with errors ranging from 0 to 45 mm and hemispheres ranging from 5 to 38 mm radius.

Fig. 6(a) could be redrawn for any of the hemispheres that we tested, and a similar improvement for the positive pressure gripper would be shown. However, we find that the expression  $\sqrt{e^2 + r^2}/R$  allows us to observe the error tolerance and reliability of the gripper more generally. This expression can be understood as the Euclidean distance from the apex of the target object to the point where the gripper touches the table along its central axis, compared with the radius of the gripper. It is a simple approximation of the total surface area the gripper will contact (table plus target object), as it attempts to wrap around the object to the critical contact angle, compared with the available surface area of the gripper. An analytical calculation of these two surface areas would likely produce a more accurate quantity, but such a calculation is prohibitively difficult because of the deformation and stretching of the gripper membrane that occurs during the gripping process. We see in Fig. 6(b) that our approximation is sufficiently simple and accurate to collapse the data and allow for quick estimations of gripping success rate. In addition, the close similarity between Figs. 5(a) and 6(b) should be noted. This result is expected because  $\sqrt{e^2 + r^2}/R$  reduces to  $r/R$  for  $e = 0$ .

The error tolerance that we observe for the jamming gripper is very large considering its open-loop function. In Fig. 6(a), for example, we see that with the use of positive pressure, our 43 mm radius gripper can successfully pick up a 25 mm radius hemisphere 100% of the time, even when the hemisphere is 25 mm away from its target location. Furthermore, the ability of jamming grippers to resist torques and off-axis forces has been previously shown [26]. It is likely that this large error tolerance would prove very useful for gripping tasks in unstructured

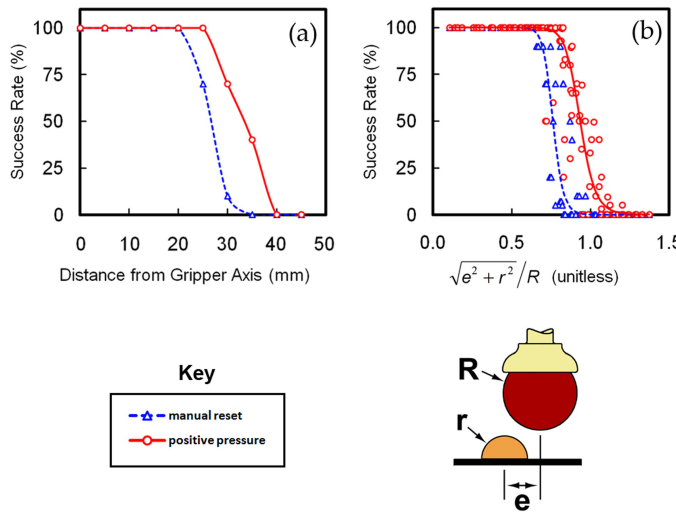


Fig. 6. Results from testing the gripper against errors in the location of the target object. (a) Error tolerance of about 30 mm as well as an increase in error tolerance and reliability can be seen for a hemisphere of 25 mm radius. (b) Error tolerance and reliability can be seen more generally for errors ranging from 0 to 45 mm and hemispheres ranging from 5 to 38 mm radius using the unitless value  $\sqrt{e^2 + r^2}/R$ .

environments, where precise control over neither the situation nor the robot is possible.

### C. Shapes and Strength

In our third test, the jamming gripper was evaluated for the range of shapes that it could grip and the forces with which it could retain those shapes. Seven shapes with similar mass, volume, and size were 3-D printed for the test. The mass of each shape was  $15.5 \pm 0.8$  g. The minimum cross section of each shape was approximately 26 mm—a size chosen to be well within the 100% success rate from the previous tests. The 3-D printed material is not smooth enough for an airtight seal to be achieved. The shapes printed were helical spring, cylinder, cuboid, jack toy, cube, sphere, and regular tetrahedron. A photograph of the shapes is shown on the ordinate of Fig. 7. To test the strength with which each object was retained, we measured the force that is required to remove a held object from the gripper. The results of this test are shown in Fig. 7. Ten tests were performed for each shape, and the error bars indicate the maximum and minimum measurements that are recorded during the tests.

It can be seen that resetting the gripper with positive pressure improves the holding force for objects that displace a larger volume of grains in the gripper but decreases the holding force for smaller objects. This may be understood as a tradeoff between contact angle and applied force in the experimental setup. The enhanced flowability of the positive pressure gripper allows for a larger contact angle, as seen in Fig. 5(c) and, thus, an enhanced holding force for the larger objects that displace a larger volume of grains. However, a problem occurs for the smaller objects because no significant increase in contact angle occurs. Instead, the enhanced flowability may allow more grains to fall to the side of the object, possibly leaving a gap between the grains and the gripper base. This is supported by the low values of applied force in Fig. 5(b) for the positive pressure gripper, which are

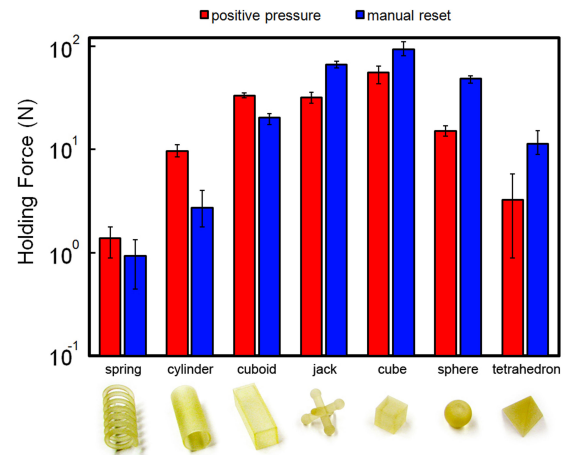


Fig. 7. Holding force for 3-D printed plastic shapes: helical spring, cylinder, cuboid, jack toy, cube, sphere, and regular tetrahedron. The sphere is 2.6 cm in diameter.

comparable with the weight of the grains for small objects. In this situation, when the membrane is evacuated, the grains may partially contract toward the open space near the gripper base rather than toward the target object, resulting in less holding force. This is not an inherent problem with the positive pressure modification, as it could be fixed by applying more force to the target object, either by adjusting the pick height  $h_1$  to the target object size or by using a robot arm with force feedback.

### D. Speed

The actuation speed of a positive pressure jamming gripper depends on the vacuum and positive pressure flow rates. These set the time required to complete the jamming transition when evacuating the gripper and the time required to reset the gripper with positive pressure. Here, we have achieved minimum actuation times of 1.1 s to evacuate the gripper and 0.1 s to reset the gripper. The 0.1 s reset time is probably near the lower limit of what is practical, as it was achieved with a standard 650 kPa compressed air line in a workshop. There is significant room for improvement, however, in the evacuation time. Faster evacuation times could be achieved by incorporating an evacuated reservoir between the pump and the valve leading to the gripper, for example, and we believe that evacuation times of the order of 0.1 s are also possible.

All of the tests in this paper were conducted at 100% joint angle speed of the robot, which was measured at 240 mm/s. We can, therefore, calculate that for the test setup shown in Fig. 4, a gripping rate of 16.2 picks/min can be achieved with the positive pressure gripper. Much higher gripping rates would be possible with a faster robot arm, for example, a delta robot.

### E. Placement Precision

Typically, placement precision is recognized as a sacrifice that must be made when developing a passive universal gripper in order to maximize the range of objects that may be gripped [1]. However, placement precision is also a key performance measure for grippers that are used in manufacturing settings. Here, the jamming gripper is evaluated for the precision and

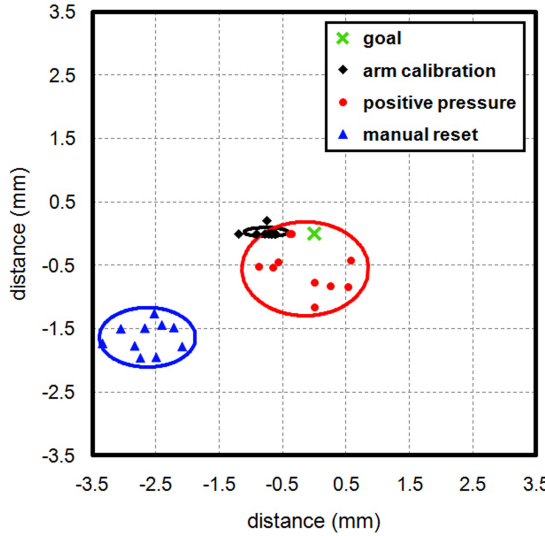


Fig. 8. Placement test results for the calibration of the robot arm, test of the positive pressure gripper, and test of the manually reset gripper. Ellipses represent 95% confidence regions.

accuracy with which it can place objects, again using the same test setup from Fig. 4 with slight modifications.

We first performed a calibration procedure to determine the precision and accuracy of the robot arm itself. A pen was firmly mounted to the wrist of the robot, extending to approximately the same point at which a fully reset gripper would make contact with the table. A similar test procedure to Fig. 4 was then executed, with the pen marking a fixed piece of paper at the pick and place positions  $P_1$  and  $P_2$ . With this setup, we were able to determine the precision of the arm to be  $\pm 0.35$  mm in the worst case for 95% confidence, with an average offset of 0.76 mm from the goal. This result is seven times larger than the manufacturers reported repeatability of  $\pm 0.05$  mm, which is likely due to the dynamic effects that are caused by moving the robot arm at full speed.

Next, the pen was removed from the robot arm, and the gripper was reattached. The robot arm was programmed to execute a pick and place routine with the hemisphere, again using the test setup from Fig. 4. Following placement of the hemisphere, we were able to measure its deviation from its intended position in the plane of the table. In this test, only the 18 mm radius hemisphere was used. This hemisphere is similar to the part sizes that are used in the shape test and is well within the 100% success rate range in the reliability test. The dimensions of Fig. 4 were slightly modified for this test: When testing the positive pressure gripper,  $h_2$  was set at 88 mm, and when testing the manually reset gripper,  $h_2$  was set at 71 mm. The results are shown in Fig. 8.

We see from Fig. 8 that the positive pressure gripper places the hemisphere more accurately than the manually reset gripper, while the manually reset gripper is slightly more precise. Specifically, the average deviation of the positive pressure gripper is 0.98 mm from the arm's calibration center, with a precision of  $\pm 1.00$  mm in the worst case for 95% confidence, while the average deviation for the manually reset gripper is 2.63 mm from

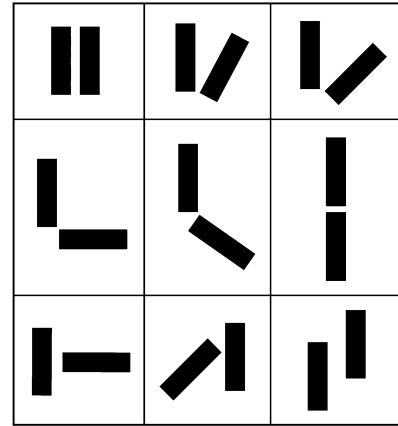


Fig. 9. Nine starting configurations that are used to test the jamming gripper's ability to grip multiple objects at once, shown from a top view.

the arm's calibration center, with a precision of  $\pm 0.76$  mm in the worst case for 95% confidence.

The precision and accuracy in angular placement is comparable between the two grippers. Here, however, the manually reset gripper slightly was more accurate, while the positive pressure gripper was slightly more precise. The manually reset gripper rotated the hemisphere by  $5.4^\circ$  on average,  $\pm 3.4^\circ$  for 95% confidence. The positive pressure gripper rotated the hemisphere by  $7.5^\circ$  on average,  $\pm 1.8^\circ$  for 95% confidence.

The placement accuracy improvement that we observe for the positive pressure jamming gripper enables repeatable shooting behavior presented later in Section III-G. It should be noted that it is not strictly necessary to apply the positive pressure exactly at the moment of object release and that releasing the object and resetting the gripper can be separated into distinct operations. If the improved placement precision of the manual reset gripper is preferred, one could calibrate for the constant offset in placement accuracy and then simply release the vacuum to drop the object and pressurize the gripper later to reset it.

#### F. Multiple Objects

A unique feature of jamming grippers is their ability to grip multiple closely spaced objects simultaneously while maintaining their relative position and orientation. An example of this was shown in Fig. 1. To quantify this capability, we used two cuboids as test parts—each  $13 \times 13 \times 45$  mm. The gripper was evaluated to pick these objects at the nine starting configurations that are shown in Fig. 9. We again implemented the test procedure from Fig. 4 with the same modifications that are specified in the placement precision test. For each test, the centroid of the combined shape was located on the central axis of the gripper. The relative distance and angle between the two objects was recorded before and after the gripping operation.

We found that for relative distance, the manually reset gripper tended to increase the separation between the objects by 0.8 mm on average,  $\pm 8.6$  mm for 95% confidence, while the positive pressure gripper tended to increase the separation between the objects by 7.7 mm on average,  $\pm 10.7$  mm for 95% confidence. In terms of relative angle, the manually reset gripper changed

the angle between the objects by  $6.7^\circ$  on average,  $\pm 20.5^\circ$  for 95% confidence, while the positive pressure gripper changed the angle between the objects by  $5.2^\circ$  on average,  $\pm 22.2^\circ$  for 95% confidence.

This test shows a significant decrease in accuracy from the previous test, where only one object was used. The increase in error is likely the result of grips that occur away from the central axis of the gripper, where off-axis forces that tend to rotate or translate the gripped objects are more likely to occur. The performance of the positive pressure gripper is slightly inferior to the manually reset gripper in this test, presumably because the rapid expansion of the membrane during the ejection of the object magnifies these off-axis forces, producing increased rotations and translations of the gripped objects. This test reveals the importance of centering objects on the gripper's central axis in order to maximize placement accuracy.

The performance of both the positive pressure gripper and the manually reset gripper in this test indicates that they can be used to grip multiple objects at once but that their ability to maintain the relative distance and angle between the objects is only suitable for tasks where a lower degree of accuracy is required. For example, this capability may be useful for transferring multiple aligned parts prior to a more accurate assembly operation.

### G. Shooting

The fast ejection of objects by positively pressurizing the gripper enables the gripper to launch or shoot objects a significant distance. Other grippers are typically unable to throw or shoot objects on their own, instead relying on the robot arm to provide the momentum for throwing. To study the shooting capability of the positive pressure jamming gripper, we developed the test that is shown in Fig. 10. The gripper picks up the object at a known location and then moves to the shooting location ( $h_4 = 290$  mm,  $\phi = 45^\circ$ ). A 0.1 s burst of pressurized air (2.16 L/s at 620 kPa) is then applied, and the shooting distance  $L$  is measured. Seven 38 mm diameter spheres weighing between 5 and 45 g were tested, along with the six additional shapes that were used in the holding force test. Results are shown in Fig. 10.

It can be seen that mass does not have a significant influence on the travel distance of ejected spheres. We can then infer that the jamming gripper acts as a velocity source rather than a force source. This is useful because it means the angle  $\phi$  is the relevant control parameter for shooting. It can also be seen that other objects tend not to travel as far as spheres. This can be explained by the increased likelihood that the ejection velocity vector is not aligned with the center of these objects and is instead partially lost in rotating the object. In addition, these nonspherical objects will likely experience increased atmospheric drag. Furthermore, the four objects that travel the shortest distance have the sharpest corners. This could indicate that a sharply bent membrane cannot relax as quickly and, thus, gives the object a lower initial velocity.

In general, for angle  $\phi = 45^\circ$  and  $h_4 = 290$  mm, objects of varying size and weight can be ejected  $602 \text{ mm} \pm 127 \text{ mm}$  with 95% confidence, which can be improved if the shape of the object is known. Precision in the perpendicular direction is

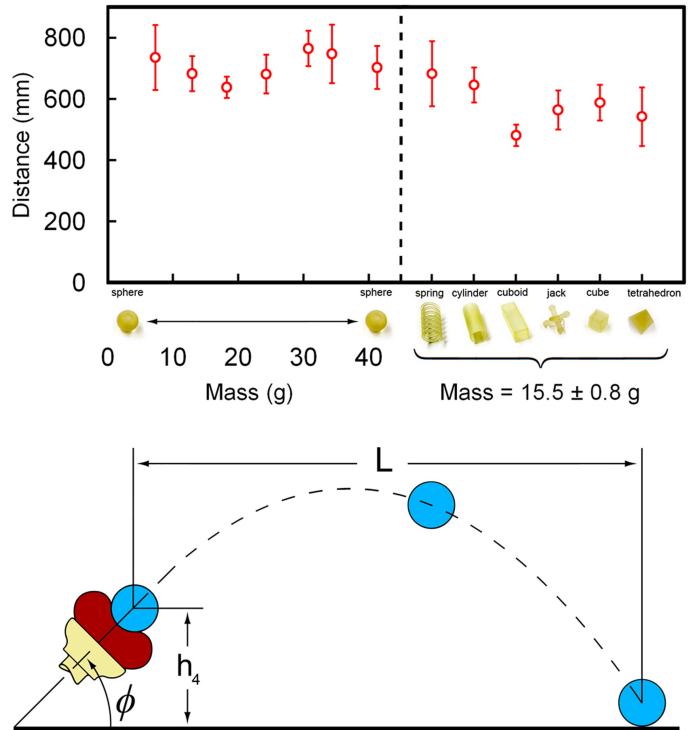


Fig. 10. Shooting test (top) results and (bottom) setup. The gripper shoots the object from angle  $\phi$  and height  $h_4$  so that distance  $L$  can be measured. Results show the shooting distance for seven spheres of varying mass and six other objects with the same mass and varying shape.

$\pm 60$  mm for 95% confidence. This is certainly too coarse for high-precision manufacturing tasks but could be useful for tasks like sorting objects into bins in a factory or throwing away trash in a home.

### IV. RELATED GRIPPERS

To compare passive- and underactuated-type universal grippers with one another is a surprisingly difficult task. Grippers in this group often derive their utility from a unique gripping approach, and this, in turn, necessitates an equally unique set of tests to demonstrate the gripper's capabilities. No standard set of benchmark tests is followed in the literature. Further, many of the references in this field focus primarily on the design, manufacturing, and control strategies that are implemented in their particular gripper and, thus, provide minimal quantitative performance data. Some of the seemingly critical performance parameters that we have presented here (especially placement precision) are mostly absent from the related literature. Finally, most all of these grippers are singular prototypes that are produced for research purposes and, therefore, cannot be obtained for further testing.

In this paper, we too have devised a customized set of tests that we believe objectively and quantitatively reveal both the capabilities and limitations of our proposed gripper. We are able to compare the positive pressure jamming gripper with other passive- and underactuated-type universal grippers, as shown in Table I. Here, the *DOF at Joints* column indicates the number of DOF at traditional joints, such as revolute or ball and

TABLE I  
COMPARISON OF PASSIVE- AND UNDERACTUATED-TYPE UNIVERSAL GRIPPERS

Gripper Name	DOF at Joints (number)	Additional Compliance (Y/N)	No. of Actuators	Object Size Range (% of size)*	Error Tolerance (% of size) <sup>†</sup>	Grip/Pinch Force (N)	Holding Force (N)	Placement Precision (mm)	Actuation Time (s)
<b>Positive Pressure Jamming Gripper</b>									
100G [34][35]	NA	Y	1	<10 - 85	≈72	~0.1 - 10	~1 - 100	±1.00	0.1 - 1.1
CAVG [7][36]	4	N	1	unknown	unknown	unknown	unknown	unknown	0.025
Keio Underactuated [37]	80	N	2	?- >100	unknown	0	unknown	unknown	unknown
Laval Underactuated [38]	15	Y	1	~human	NA	25-65	10-50	NA	0.8
Omnigripper [6]	15	N	1	~human	unknown	2.5	40	unknown	unknown
RTR II [39][40]	255	N	1	≈1-90	<50	unknown	19.6	unknown	unknown
SARAH [16][17][18]	9	N	2	unknown	NA	4-20	≈1-5	NA	unknown
SDM Hand [13][14][15]	10	Y	1	?-120	unknown	67-222	>267	unknown	3.5
Soft Gripper [11][12]	8	N	2	?-125	≈47	30	unknown	unknown	unknown
SPRING hand [41]	18	N	1	unknown	unknown	0.2 N/cm	unknown	unknown	unknown
Starfish gripper [8]	8	N	1	~human	NA	5-10	≈1	NA	unknown
TBM Hand [42]	NA	Y	1	≈17-83	unknown	unknown	≈0.5-3	unknown	unknown
TUAT/Karlsruhe [43]	20	N	1	~human	unknown	unknown	unknown	NA	4-5

\* $r/R$ ; <sup>†</sup> $e/R$  for  $r/R \approx 0.5$  ( $r$ ,  $R$ , and  $e$  are defined in Fig. 6).

socket joints. Flexural joints or members that can bend, stretch, or twist in multiple directions are included in the *Additional Compliance* column. The *Object Size Range* column specifies the range of objects that the gripper can pick up. This is normalized to the gripper size by dividing approximate object radius by approximate gripper radius ( $r/R$ ). If the gripper is a five-fingered hand based closely on the dimensions of a human hand, then we replace otherwise unreported size ranges with  $\sim$ human. The *Error Tolerance* column is also normalized to the gripper size using an object with approximately half the radius of the gripper. With this constant object size, error tolerance is the maximum tolerable error in object location divided by gripper radius ( $e/R$ ). For grippers that are intended specifically for prosthetic uses, we replace unreported values in the *Error Tolerance* and *Placement Precision* columns with NA, as these are typically the responsibility of the prosthesis operator rather than the hand itself. Any values that are not specifically reported in the literature but that could be closely estimated were added to the table.

We have limited our survey to grippers that have two actuators or less and at least three times as many DOF as actuators. We believe this is the appropriate bound for comparison because at the cutoff, it includes multifingered hands such as SARAH [16]–[18], which have some meaningful similarities in the area of shape adaptation, but it excludes others like the Barrett Hand [33], which are more highly actuated and with which a comparison would have little utility. This survey is not exhaustive (particularly, in the area of prosthetics and five-fingered hands) but serves to illustrate the trend of underreported and unknown performance metrics in the related literature. We hope that the performance-centric approach of this paper will provide some new benchmarks for future work in the field.

From Table I, we can see that the positive pressure jamming gripper is the top performer in both error tolerance and placement precision, and its performance on the remaining tests is also very good. There is no column in which the positive pressure jamming gripper is an obvious underperformer. These re-

sults further support the potential adoption of universal jamming grippers for tasks where low complexity but high versatility are required.

## V. CONCLUSION

In this paper, we have presented a passive universal jamming gripper that incorporates both positive and negative pressure. The design and manufacture of a prototype gripper were described, and this prototype was evaluated against five metrics that revealed its capabilities for real-world applications. The positive pressure gripper proved capable at gripping objects of different size and shape, and when compared with a version without positive pressure, it showed an increase in reliability of up to 85% and an increase in error tolerance of up to 25%. The positive pressure gripper also applied up to 90% less force on target objects, demonstrated an increase in placement accuracy, and was able to extend its workspace up to 600 mm by shooting objects. This ability to manipulate objects by shooting may be useful for tasks like sorting objects into bins in a factory or throwing away trash in a home.

With this jamming gripper, objects of very different shape, weight, and fragility can be gripped, and multiple objects can be gripped at once while maintaining their relative distance and orientation. This diversity of abilities may make the gripper well suited for use in unstructured domains ranging from military environments to the home and, perhaps, for variable industrial tasks, such as food handling. The gripper's airtight construction also provides the potential for use in wet or volatile environments and permits easy cleaning. Its thermal limits are determined only by the latex rubber membrane, because of the temperature independence of the jamming phase transition; therefore, use in high- or low-temperature environments may also be possible with a modified design. Furthermore, the soft malleable state that the gripper assumes between gripping tasks could provide an improvement in safety when deployed in close proximity with humans, as in the home, for example.

The durability of a single latex membrane could be a concern, and we believe that future work in this area will lead to improved membrane materials. It should be noted, however, that throughout our several hundreds of tests conducted for this paper, the latex membrane never failed and showed no visible signs of wear.

We have demonstrated a jamming-based gripper with a number of unique capabilities and adept performance. However, the gripper that is presented here is still a fairly early prototype. We believe that significant performance gains are possible and that further research will serve to optimize the gripper membrane, jamming material, and overall design to produce a gripper that far surpasses the capabilities and performance that are demonstrated here.

## REFERENCES

- [1] D. T. Pham and S. H. Yeo, "Strategies for gripper design and selection in robotic assembly," *Int. J. Prod. Res.*, vol. 29, pp. 303–316, Feb. 1991.
- [2] A. Bicci and V. Kumar, "Robotic grasping and contact: A review," in *Proc. IEEE Int. Conf. Robot. Autom.*, Apr., 2000, pp. 348–353.
- [3] A. T. Miller, S. Knoop, P. K. Allen, and H. I. Christensen, "Automatic grasp planning using shape primitives," in *Proc. IEEE Int. Conf. Robot. Autom.*, Sep., 2003, pp. 1824–1829.
- [4] K. B. Shimoga, "Robot grasp synthesis algorithms: A survey," *Int. J. Robot. Res.*, vol. 15, pp. 230–266, Jun. 1996.
- [5] A. Saxena, J. Driemeyer, and A. Y. Ng, "Robotic grasping of novel objects using vision," *Int. J. Robot. Res.*, vol. 27, pp. 157–173, Feb. 2008.
- [6] P. B. Scott, "The 'Omnigripper': A form of robot universal gripper," *Robotica*, vol. 3, pp. 153–158, Sep. 1985.
- [7] R. Tella, J. Birk, and R. Kelley, "A contour-adapting vacuum gripper," in *Robot Grippers*, D. T. Pham and W. B. Heginbotham, Eds. New York: Springer-Verlag, 1986, pp. 86–100.
- [8] F. Ilievski, A. D. Mazzeo, R. F. Shepherd, X. Chen, and G. M. Whitesides, "Soft robotics for chemists," *Angewandte Chemie International Edition*, vol. 50, pp. 1890–1895, Feb. 2011.
- [9] D. H. Wolpert and W. G. Macready, "No free lunch theorems for optimization," *IEEE Trans. Evol. Comput.*, vol. 1, no. 1, pp. 67–82, Apr. 1997.
- [10] L. Birglen, T. Laliberté, and C. Gosselin, *Underactuated Robotic Hands*. Berlin, Germany: Springer-Verlag, 2008.
- [11] S. Hirose and Y. Umetani, "The development of soft gripper for the versatile robot hand," *Mech. Mach. Theory*, vol. 13, pp. 351–359, 1978.
- [12] S. Hirose, "Connected differential mechanism and its applications," in *Robot Grippers*, D. T. Pham and W. B. Heginbotham, Eds. New York: Springer-Verlag, 1986, pp. 141–153.
- [13] A. M. Dollar and R. D. Howe, "A robust compliant grasper via shape deposition manufacturing," *IEEE/ASME Trans. Mechatron.*, vol. 11, no. 2, pp. 154–161, Apr. 2006.
- [14] A. M. Dollar and R. D. Howe, "Simple, robust autonomous grasping in unstructured environments," in *Proc. IEEE Int. Conf. Robot. Autom.*, Apr. 2007, pp. 4693–4700.
- [15] A. M. Dollar and R. D. Howe, "The SDM Hand as a prosthetic terminal device: A feasibility study," in *Proc. IEEE Int. Conf. Rehabil. Robot.*, Jun., 2007, pp. 978–983.
- [16] T. Laliberté and C. Gosselin, "Underactuation in space robotic hands," in *Proc. 6th Int. Symp. Artif. Intell., Robot., Autom. Space*, Jun. 2001.
- [17] T. Laliberté, L. Birglen, and C. Gosselin, "Underactuation in robotic grasping hands," *Mach. Intell. Robot. Control*, vol. 4, pp. 1–11, Sep. 2002.
- [18] B. Rubinger, M. Brousseau, J. Lymer, C. Gosselin, T. Laliberté, and J. C. Piedboeuf, "A novel robotic hand-SARAH for operations on the International Space Station," in *Proc. 7th Workshop Adv. Space Technol. Robot. Autom.*, Nov. 2002.
- [19] H. J. Warnecke and I. Schmidt, "Flexible gripper for handling systems: Design possibilities and experiences," *Int. J. Prod. Res.*, vol. 18, pp. 525–537, Sep./Oct. 1980.
- [20] P. K. Wright and M. R. Cutkosky, "Design of grippers," in *Handbook of Industrial Robotics*, S. F. Nof, Ed. New York: Wiley, 1985, pp. 91–111.
- [21] H. Choi and M. Koc, "Design and feasibility tests of a flexible gripper based on inflatable rubber pockets," *Int. J. Mach. Tools Manuf.*, vol. 46, pp. 1350–1361, Oct. 2006.
- [22] D. C. Simpson, "Gripping surfaces for artificial hands," *Hand*, vol. 3, pp. 12–14, Feb. 1971.
- [23] I. Schmidt, "Flexible moulding jaws for grippers," *Ind. Robot*, vol. 5, pp. 24–26, Mar. 1978.
- [24] A. P. Perovskii, "Universal grippers for industrial robots," *Russian Eng. J.*, vol. 60, pp. 9–11, Aug. 1980.
- [25] T. Reinmuller and H. Weissmantel, "A shape adaptive gripper finger for robots," *Proc. Int. Symp. Ind. Robots*, pp. 241–250, Apr. 1988.
- [26] E. Brown, N. Rodenberg, J. Amend, A. Mozeika, E. Steltz, M. Zakin, H. Lipson, and H. Jaeger, "Universal robotic gripper based on the jamming of granular material," *Proc. Nat. Acad. Sci.*, Nov. 2010, vol. 107, pp. 18809–18814.
- [27] T. S. Majmudar, M. Sperl, S. Luding, and R. P. Behringer, "Jamming transition in granular systems," *Phys. Rev. Lett.*, vol. 98, pp. 058001–058004, Feb. 2007.
- [28] A. J. Liu and S. R. Nagel, "Jamming is not just cool any more," *Nature*, vol. 396, pp. 21–22, Nov. 1998.
- [29] M. E. Cates, J. P. Wittmer, J. P. Bouchaud, and P. Claudin, "Jamming, force chains, and fragile matter," *Phys. Rev. Lett.*, vol. 81, pp. 1841–1844, Aug. 1998.
- [30] A. J. Liu and S. R. Nagel, *Jamming and Rheology: Constrained Dynamics on Microscopic and Macroscopic Scales*. London, U.K.: Taylor & Francis, 2001.
- [31] C. S. O'Hern, L. E. Silbert, A. J. Liu, and S. R. Nagel, "Jamming at zero temperature and zero applied stress: The epitome of disorder," *Phys. Rev. E*, vol. 68, pp. 011306–011336, Jul. 2003.
- [32] E. I. Corwin, H. M. Jaeger, and S. R. Nagel, "Structural signature of jamming in granular media," *Nature*, vol. 435, pp. 1075–1078, Apr. 2005.
- [33] W. Townsend, "The BarrettHand grasper—Programmably flexible part handling and assembly," *Ind. Robot*, vol. 27, pp. 181–188, 2000.
- [34] M. Kaneko, M. Higashimori, R. Takenaka, A. Namiki, and M. Ishikawa, "The 100 G capturing robot—Too fast to see," *IEEE/ASME Trans. Mechatronics*, vol. 8, no. 1, pp. 37–44, Mar. 2003.
- [35] M. Higashimori, M. Kaneko, A. Namiki, and M. Ishikawa, "Design of the 100G capturing robot based on dynamic preshaping," *Int. J. Robot. Res.*, vol. 24, pp. 743–753, Sep. 2005.
- [36] R. Tella, J. R. Birk, and R. B. Kelley, "General purpose hands for bin-picking robots," *IEEE Trans. Syst., Man, Cybern.*, vol. SMC-12, no. 6, pp. 828–837, Nov./Dec. 1982.
- [37] Y. Kamikawa and T. Maeno, "Underactuated five-finger prosthetic hand inspired by grasping force distribution of humans," in *Proc. IEEE/RSJ Int. Conf. Intell. Robots Syst.*, Sep. 2008, pp. 717–722.
- [38] C. Gosselin, F. Pelletier, and T. Laliberté, "An anthropomorphic underactuated robotic hand with 15 DOFs and a single actuator," in *Proc. IEEE Int. Conf. Robot. Autom.*, May 2008, pp. 749–754.
- [39] B. Massa, S. Roccella, M. C. Carrozza, and P. Dario, "Design and development of an underactuated prosthetic hand," in *Proc. IEEE Int. Conf. Robot. Autom.*, May 2002, vol. 4, pp. 3374–3379.
- [40] M. C. Carrozza, F. Vecchi, F. Sebastiani, G. Cappiello, S. Roccella, M. Zecca, R. Lazzarini, and P. Dario, "Experimental analysis of an innovative prosthetic hand with proprioceptive sensors," in *Proc. IEEE Int. Conf. Robot. Autom.*, Sep. 2003, vol. 2, pp. 2230–2235.
- [41] M. C. Carrozza, C. Suppo, F. Sebastiani, B. Massa, F. Vecchi, R. Lazzarini, M. R. Cutkosky, and P. Dario, "The SPRING hand: Development of a self-adaptive prosthesis for restoring natural grasping," *Auton. Robots*, vol. 16, pp. 125–141, Mar. 2004.
- [42] N. Dechev, W. L. Cleghorn, and S. Naumann, "Multiple finger, passive adaptive grasp prosthetic hand," *Mech. Mach. Theory*, vol. 36, pp. 1157–1173, Oct. 2001.
- [43] N. Fukaya, S. Toyama, T. Asfour, and R. Dillmann, "Design of the TUAT/Karlsruhe humanoid hand," in *Proc. IEEE/RSJ Int. Conf. Intell. Robots Syst.*, Oct./Nov. 2000, vol. 3, pp. 1754–1759.



**John R. Amend, Jr.** (S'10) received the B.S. degree in mechanical engineering from the State University of New York at Buffalo (SUNY Buffalo) in 2008. He is currently working toward the Ph.D. degree with the Creative Machines Lab, Cornell University, Ithaca, NY.

In 2007 and 2008, he was involved in research activities with the Automation Robotics and Mechatronics Laboratory, and the Design of Open Engineering Systems Laboratory, both at SUNY Buffalo. His current research interests include using controlled granular jamming for physically adaptive robots.

Mr. Amend is a Student Member of the American Society of Mechanical Engineers and the American Society for Engineering Education, as well as a National Science Foundation Graduate Research Fellowship recipient.



**Eric Brown** was born in Wilmington, DE. He received the B.S. degree in physics from Harvey Mudd College, Claremont, CA, in 2002 and the Ph.D. degree in physics from the University of California, Santa Barbara, in 2007.

He is currently an Assistant Professor with the School of Natural Sciences, University of California, Merced. He was a Postdoctoral Scholar with the James Franck Institute, The University of Chicago, Chicago, IL. His current research interests include rheology, granular materials, and turbulence.

Dr. Brown is a member of the American Physical Society and the Society of Rheology.



**Heinrich M. Jaeger** received the Vordiplom degree in physics from the University of Kiel, Kiel, Germany, in 1979 and the Ph.D. degree in physics from the University of Minnesota, Minneapolis, in 1987.

He is currently the William J. Friedman and Alicia Townsend Professor of physics with the University of Chicago, Chicago, IL. On the faculty with the University of Chicago since 1991, he has been a Director of the Chicago Materials Research Science and Engineering Center and of the James Franck Institute. His

current research interests focus on using particle assemblies, from nanoparticles to macroscopic granular matter, for the design of functional materials.



**Nicholas Rodenberg** received the B.A. degree in physics from the University of Chicago, Chicago, IL, in 2010.

He is currently a Robotic Technician for the LS3 Program with Boston Dynamics, Waltham, MA. He performed research as an undergraduate with the University of Chicago under Dr. H. Jaeger in the fields of granular behavior and materials science. He spent five years as a Helicopter Mechanic in the United States Marine Corps.



**Hod Lipson** (M'98) received the B.Sc. degree in mechanical engineering and the Ph.D. degree in mechanical engineering in computer-aided design and artificial intelligence in design from the Technion–Israel Institute of Technology, Haifa, Israel, in 1989 and 1998, respectively.

He is currently an Associate Professor with the Sibley School of Mechanical and Aerospace Engineering and Computing and Information Science, Cornell University, Ithaca, NY. He was a Postdoctoral Researcher with the Department of Computer Science, Brandeis University, Waltham, MA. He was a Lecturer with the Department of Mechanical Engineering, Massachusetts Institute of Technology, Cambridge, where he was involved in conducting research in design automation. His current research interests include computational methods to synthesize complex systems out of elementary building blocks and the application of such methods to design automation and their implication toward understanding the evolution of complexity in nature and in engineering.